

Failure Mechanisms of Graphene under Tension

C. A. Marianetti¹ and H. G. Yevick²

¹*Department of Applied Physics and Applied Mathematics, Columbia University, New York, New York 10027, USA*

²*Department of Physics, Columbia University, New York, New York 10027, USA*

(Received 4 August 2010; published 10 December 2010)

Recent experiments established pure graphene as the strongest material known to mankind, further invigorating the question of how graphene fails. Using density functional theory, we reveal the mechanisms of mechanical failure of pure graphene under a generic state of tension at zero temperature. One failure mechanism is a novel soft-mode phonon instability of the K_1 mode, whereby the graphene sheet undergoes a phase transition and is driven towards isolated hexagonal rings resulting in a reduction of strength. The other is the usual elastic instability corresponding to a maximum in the stress-strain curve. Our results indicate that finite wave vector soft modes can be the key factor in limiting the strength of monolayer materials.

DOI: [10.1103/PhysRevLett.105.245502](https://doi.org/10.1103/PhysRevLett.105.245502)

PACS numbers: 61.48.Gh, 62.25.-g, 63.22.Rc, 64.70.Nd

The mechanical failure of materials is usually a complex process which may involve defects at a variety of length scales, such as dislocations, grain boundaries, cracks, etc. The complexity and statistical nature of these defects cause mechanical failure to be extremely dependent on not only the type of material but also on the manner in which the material was synthesized. To the contrary, ideal strength, which can be defined as the maximum attainable stress under a uniform strain field in the absence of any instabilities, is an intrinsic property of a material [1]. Recently, the measurement of ideal strength has been achieved in the case of graphene [2], a monolayer of carbon. Using nanoindentation, Lee *et al.* strained graphene until failure under conditions which appear to be very nearly ideal [3]. This experiment reinvigorates the fundamental question of how and why a material fails under ideal conditions. The answer lies within the forces which bond a material together. Computing these forces from the first principles of quantum mechanics is made possible by intelligent approximations to the quantum many-body problem, such as the local density approximation (LDA) of density functional theory (DFT) [4], in addition to plentiful computational resources. While LDA may qualitatively break down in certain situations where the electronic correlations are strong [5], it works reliably in materials with relatively large electronic bands such as graphene. Although quantitative errors are still to be expected, in the vicinity of 10% for certain phonons of graphene [6,7], one can reliably explore the mechanical properties of graphene from first principles. In this study, we use DFT to determine the mechanism of mechanical failure for an arbitrary state of tension at zero temperature.

Perhaps the simplest instability is the so-called elastic instability, whereby a maximum in the stress-strain relation is achieved while retaining the symmetry of strained lattice. To determine the elastic instability of a material, DFT can be used to generate the forces as a function of strain, and such studies were performed once sufficient

computational power was available (see Ref. [8] and references therein). However, there is no guarantee that the structure will remain stable with respect to *inhomogeneous* deformations under strain. In order to determine if a structure is mechanically stable, one needs to confirm that all of the phonon energies are real and positive [9]. Phonon modes with zero or very small energies, excluding the acoustic phonons for $k \rightarrow 0$, are usually termed “soft modes” [10]. There are numerous structural phase transitions in which the two phases are directly connected by a soft mode, and the concept of the soft mode gained prominence in the context of elucidating the ferroelectric transition in BaTiO₃ [11,12]. In this work, we demonstrate that a soft mode is responsible for a phase transition and the resulting mechanical failure of graphene in certain states of tension. Previous DFT studies of *bulk* systems such as Al [13] and Si [14] have demonstrated that nontrivial acoustic phonon instabilities may precede the usual elastic instability for certain states of strain and therefore limit the ideal strength of the material. However, these scenarios are extremely difficult to decipher experimentally, even indirectly, due to defects and plastic deformation, while our predictions in graphene may be directly tested experimentally. Furthermore, our results on graphene yield an optical phonon instability, as opposed to the acoustic instability observed previously in bulk systems.

In the case of graphene, previous phonon calculations have determined that the elastic instability is the mechanism of failure for uniaxial strain in the armchair or zigzag directions [15] [i.e., x and y directions in Figs. 2(b) and 2(c), respectively]. Another study fit third order elastic constants to empirical tight-binding calculations [16], but this elastic parametrization cannot account for inhomogeneous instabilities revealed by the phonons. Therefore, the mode of failure in a general state of tension has never been considered. We compute the phonons using the displacement method [17], where the forces are generated using DFT within the

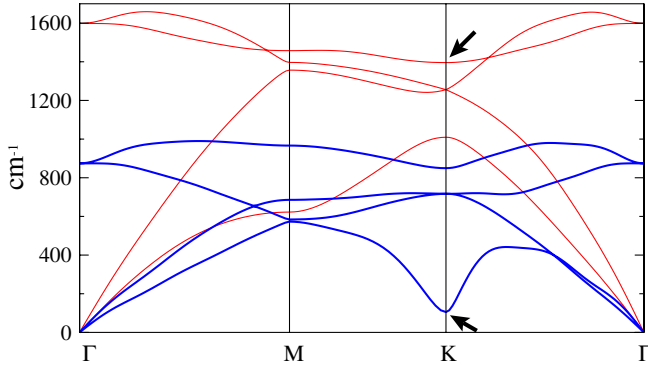


FIG. 1 (color online). The in-plane phonons of graphene under equibiaxial strain. Thin red lines and thick blue lines correspond to $\epsilon_A = 0$ and $\epsilon_A = 0.205$, respectively. A black arrow is used to identify the K_1 mode. The k point labels Γ, M, K correspond to $(0, 0), (0.5, 0), (1/3, 1/3)$, respectively, in fractions of the reciprocal lattice vectors.

local density approximation. All DFT calculations were performed using the Vienna *ab initio* simulation program (VASP) [18]. A primitive cell of $\vec{a}_1 = (a\sqrt{3}/2, -a/2)$, $\vec{a}_2 = (0, a)$ was used, where a is the nearest-neighbor bond length. An energy cutoff of 375 eV was used throughout with the soft VASP carbon projector augmented wave [19], and k -point mesh densities corresponding to a 27×27 mesh in the primitive cell were maintained. Supercells of 9×9 times the primitive cell were used when computing the force constants. Previous work has established that the displacement method is accurate for unstrained graphene [20] when using a 8×8 supercell to generate the force constants. A state of strain was constructed by applying the nominal strain $\epsilon_i = \ell_i/\ell_{i0} - 1$ and allowing all cell internal coordinates to relax.

In Fig. 1, we reproduce the phonons for unstrained graphene, showing excellent agreement with previous work [15,20]. Out-of-plane phonons are not shown as they weakly depend on strain. In Fig. 1, the phonons are also shown for the case of an equibiaxial strain of $\epsilon_A = (\epsilon_x + \epsilon_y)/\sqrt{2} = 0.205$. A significant softening of the in-plane phonons is observed, which is to be expected given that all the in-plane distances are increasing uniformly. In particular, the K_1 mode at the K point has rapidly dropped towards zero. An additional phonon calculation at a strain of $\epsilon_A = 0.212$ (not pictured) indicates that the K_1 mode has become imaginary resulting in a soft mode. This implies that the structure has become unstable and will undergo a phase transition by distorting along the K_1 mode. Group theory alone dictates the nature of this K_1 mode, and by considering linear combinations of both K and K' one arrives at two distinct real distortions [21] [see Figs. 2(b) and 2(c)]. These modes can be classified as the A_1 and B_1 irreducible representations of the C_{6v} point group. While the A_1 and B_1 modes transform differently under C_{6v} , these modes form a twofold representation when including the lattice translations. Below we show the positive A_1 mode is most energetically favorable when including anharmonicity.

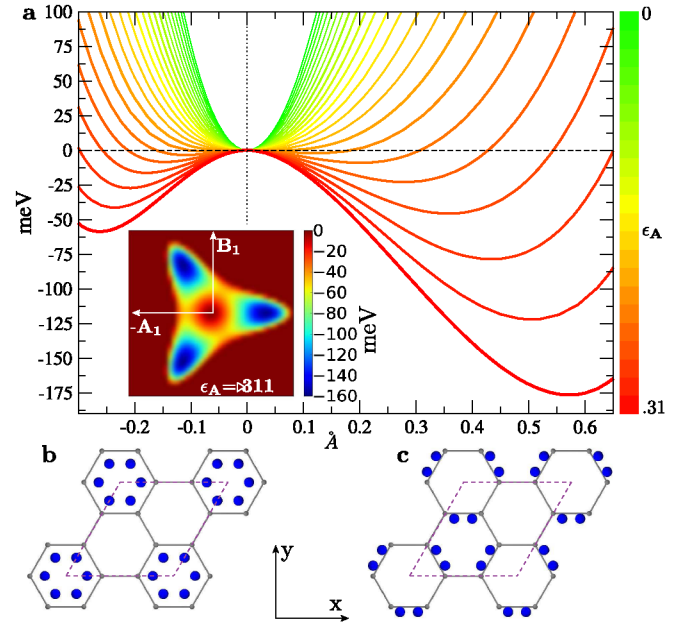


FIG. 2 (color online). (a) The energy as a function of the A_1 phonon amplitude for equibiaxial strain $\epsilon_A = (\epsilon_x + \epsilon_y)/\sqrt{2} = 0-0.311$ in increments of $\sqrt{2}/100$. The line color changes from green to yellow to red and thickness increases with increasing strain. The inset of panel (a) is a contour plot of the energy versus the A_1 and B_1 phonon amplitudes for a strain of $\epsilon_A = 0.311$. (b),(c) The positive A_1 and B_1 phonon modes, respectively (B_1 mode is symmetric). The undistorted lattice is shown in gray. The unit cell of the distorted structure (i.e., the K cell) is denoted with dotted purple lines. For illustrative purposes, the amplitudes shown corresponds to 2.5 times the amplitude for the respective well minima and $\epsilon_A = 0.311$.

One can directly explore the properties of the K_1 mode with a 6-atom unit cell, which is 3 times the size of the primitive cell [see Figs. 2(b) and 2(c)]. We shall refer to this enlarged unit cell as the K cell hereafter. The energy is computed as a function of the amplitude of the A_1 mode at a series of different equibiaxial strains [see Fig. 2(a)]. As the strain is increased, the mode continually becomes softer and eventually the curvature at zero amplitude goes to zero and the mode becomes soft. This analysis predicts the soft mode to occur at $\epsilon_A = 0.213$, independently confirming the results of our phonons which yield a soft mode at $\epsilon_A = 0.205-0.212$. Further strain results in a double-well potential, where the well depth and amplitude increase with increasing strain. One can also consider the energy in the two dimensional space of the A_1 and B_1 modes at a given strain [see Fig. 2(a) inset], and this results in the usual “warped Mexican hat” potential.

It should be emphasized that at this point one does not know if the material will fracture, only that a phase transition will occur. Therefore, we must explore the strength and stability of this new phase of strained graphene. The stress as a function of the equibiaxial strain is computed for both the primitive unit cell and the K cell (see Fig. 3). For the primitive cell, the curve is smooth and the elastic

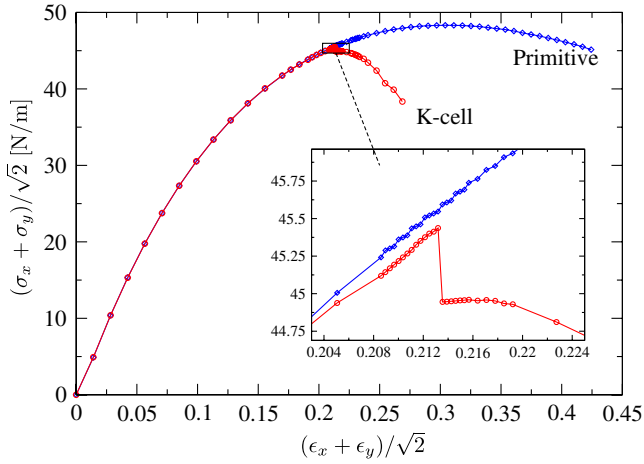


FIG. 3 (color online). Nominal stress versus equibiaxial strain. The blue line corresponds to the primitive cell and the red line to the K cell. The inset shows a magnified view of where the K_1 mode goes soft, as indicated by a discontinuity in the curve.

instability occurs at a strain of $\epsilon_A = (\epsilon_x + \epsilon_y)/\sqrt{2} = 0.307$. However, the primitive unit cell does not have the freedom to distort along the K_1 mode as the primitive translational symmetry is enforced in the calculation. The same curve can now be analyzed for the K cell. The phonon instability is clearly illustrated by a discontinuity in the curve at $\epsilon_A = 0.213$ (see inset of Fig. 3), in excellent agreement with our preceding two calculations. Upon activation of the K_1 mode, the force rapidly drops, and is subsequently nearly flat until decreasing. Therefore, this new phase which forms is essentially mechanically unstable, and there is no need to recompute the phonons for this new phase. As a result, the soft K_1 mode can be seen not only as the precursor to a phase transition as in soft-mode theory, but also as a soft-mode which leads directly to mechanical failure.

The above analysis has revealed that for equibiaxial strain the mode of failure of graphene is radically different than the usual elastic instability which is observed for uniaxial strain in the zigzag or armchair directions. Therefore, the question arises as to when the elastic instability is the failure mode versus the K_1 -mode instability for a generic state of tension. In order to resolve this we have computed the strain at maximum stress for both the primitive unit cell and the K cell, as above, for all possible linear combinations of tensile strain in the zigzag and armchair directions (see Fig. 4). As shown in Fig. 4, the plot is naturally separated into three regions. In the first and third regions the elastic instability precedes the K_1 mode instability, and therefore the failure mechanism is the elastic instability. On the contrary, in the second region the K_1 -mode instability occurs first and therefore limits the strain and strength of the material. The stress in the x and y directions at failure [i.e., along the K -cell line in Fig. 4(a)] is plotted as a function of θ [see Fig. 4(b)], indicating the stress necessary to realize the state of strain at failure.

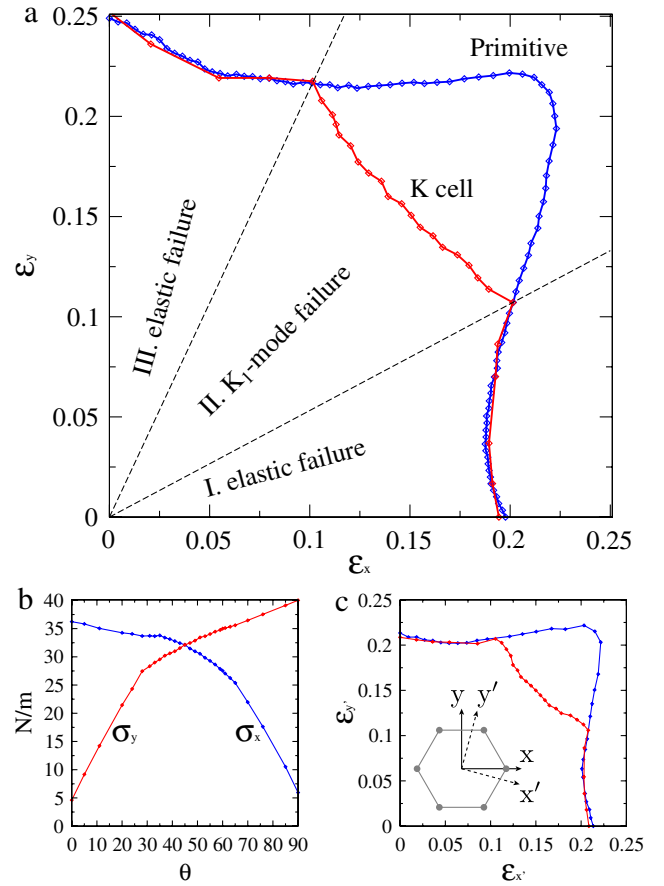


FIG. 4 (color online). (a) The maximum stable strain for the primitive unit cell (blue curve) and the K cell (red curve) as a function of all possible linear combinations of zigzag and armchair uniaxial tensile strains. A given direction of strain corresponds to an angle $\theta = 0-90$. (b) The nominal stress in the x and y directions for all points along the K -cell curve in (a). (c) The same as (a), except uniaxial strains are applied in the x' and y' directions, which correspond to a 15° rotation of the coordinate system.

This analysis is not yet exhaustive due to the fact that graphene is anisotropic, and therefore shear strain would have to be included in the present coordinate system to enumerate every possible state of tension. Alternatively, one could repeat the above analysis for every possible rotation of the coordinate system which is not generated by a member of the point group of graphene. This corresponds to generating Fig. 4(a) for every possible rotation of the coordinate system between 0° and 15° . We have rotated the coordinate system in 3° increments and regenerated Fig. 4(a) at each increment [see Fig. 4(c) for 15° rotation). Conveniently, all of the results for the different rotations are bounded by the envelope curves created by superimposing the original result and the 15° rotation. All rotation curves progress monotonically with rotation between the limits of the envelope. It should be noted that Fig. 4(c) is symmetric about $\theta = 45$ due to a mirror line which maps $x' \leftrightarrow y'$. In summary, shear strain does not

introduce any qualitative changes, and even the quantitative changes are very small for the onset of the K_1 -mode instability.

Our prediction of the soft K_1 mode may be directly verified experimentally by measuring the phonon dispersion as a function of strain. Electrons have been used to measure the surface phonons of graphite, using both reflection electron-energy-loss spectroscopy [22] and high-resolution electron-energy-loss spectroscopy [23]. Therefore, the phonons could potentially be measured directly for graphene. The challenge in this particular case would be the fact that the graphene would have to be strained *in situ*. Another more indirect probe would be Raman spectroscopy [21], which has already been performed for graphene under uniaxial tension [24] in the regime of small strains.

It is instructive to compare our results to the nanoindentation experiments of Lee *et al.* [3]. They estimated a Lagrangian breaking strain of $\epsilon_x = \epsilon_y = 0.250$, which corresponds to a nominal strain of $\epsilon_x = \epsilon_y = 0.225$. Unexpectedly, this far exceeds the breaking strain as dictated by the K_1 mode of $\epsilon_x = \epsilon_y = 0.151$. Therefore, it is clear that theory and experiment are not operating under identical conditions, and it is necessary to detail all significant differences. First, our calculations are performed at zero temperature, while the experiments are performed at room temperature. Second, the experiment could be influenced by the presence of the nanoindenter tip or other elements which may react with the graphene layer. Finally, the experiment is assumed to be in a state of equibiaxial strain while our calculations are by construction. Any and all of these differences may be linked to the difference between theory and experiment. Naively, one would expect theory to overpredict the maximum strain given that impurities may be present in the experiment or defects may be nucleated via thermal fluctuations which are not included in our simulations. However, we have shown the exact opposite to be true, and therefore this discrepancy is an anomaly. Given that LDA overpredicts the energy of the K_1 mode in the unstrained case [6,7], the exact result is likely to yield an even smaller breaking strain even farther from the experimental value. Interestingly, the results of Lee *et al.* are in much better agreement with our results for the elastic instability of equibiaxial strain (i.e., $\epsilon_x = \epsilon_y = 0.216$). This is suggestive that perhaps somehow the K_1 mode is being stabilized in the nanoindentation experiment due to one of the differences outlined above. This issue can be resolved by bridging theory and experiment in future work. Nanoindentation experiments may be performed at low

temperatures, and molecular dynamics simulations may be performed at high temperature and in a geometry similar to experiment.

In conclusion, we have determined the failure mechanisms of pure graphene in a generic state of tension at zero temperature. The usual elastic instability causes failure for strains near uniaxial while a novel soft-mode phonon instability of the K_1 mode causes failure for strains near equibiaxial. Further experiments have been suggested to directly test our prediction of the softening of the K_1 mode.

We gratefully acknowledge support from NSF via Grant No. CMMI-0927891. We thank J. W. Kysar, M. E. Manley, and J. Hone for fruitful conversations.

-
- [1] T. Zhu *et al.*, MRS Bull. **34**, 167 (2009).
 - [2] A. K. Geim and K. S. Novoselov, Nature Mater. **6**, 183 (2007).
 - [3] C. Lee *et al.*, Science **321**, 385 (2008).
 - [4] W. Kohn and L.J. Sham, Phys. Rev. **140**, A1133 (1965).
 - [5] G. Kotliar *et al.*, Rev. Mod. Phys. **78**, 865 (2006).
 - [6] A. Gruneis *et al.*, Phys. Rev. B **80**, 085423 (2009).
 - [7] M. Lazzeri *et al.*, Phys. Rev. B **78**, 081406 (2008).
 - [8] J. W. Morris and C.R. Krenn, Philos. Mag. A **80**, 2827 (2000).
 - [9] M. T. Dove, *Introduction to Lattice Dynamics* (Cambridge University Press, New York, 2005).
 - [10] J.D. Axe and G. Shirane, Phys. Today **26**, No. 9, 32 (1973).
 - [11] W. Cochran, Adv. Phys. **9**, 387 (1960).
 - [12] V.L. Ginzburg, Phys. Usp. **44**, 1037 (2001).
 - [13] D.M. Clatterbuck *et al.*, Phys. Rev. Lett. **91**, 135501 (2003).
 - [14] S.M.-M. Dubois *et al.*, Phys. Rev. B **74**, 235203 (2006).
 - [15] F. Liu, P.M. Ming, and J. Li, Phys. Rev. B **76**, 064120 (2007).
 - [16] E. Cadelano *et al.*, Phys. Rev. Lett. **102**, 235502 (2009).
 - [17] A. VandeWalle and G. Ceder, Rev. Mod. Phys. **74**, 11 (2002).
 - [18] G. Kresse and J. Furthmuller, Comput. Mater. Sci. **6**, 15 (1996).
 - [19] G. Kresse and D. Joubert, Phys. Rev. B **59**, 1758 (1999).
 - [20] O. Dubay and G. Kresse, Phys. Rev. B **69**, 089906(E) (2004).
 - [21] D.M. Basko and I.L. Aleiner, Phys. Rev. B **77**, 041409 (2008).
 - [22] C. Oshima *et al.*, Solid State Commun. **65**, 1601 (1988).
 - [23] S. Siebentritt *et al.*, Surf. Rev. Lett. **5**, 427 (1998).
 - [24] M. Y. Huang *et al.*, Proc. Natl. Acad. Sci. U.S.A. **106**, 7304 (2009).